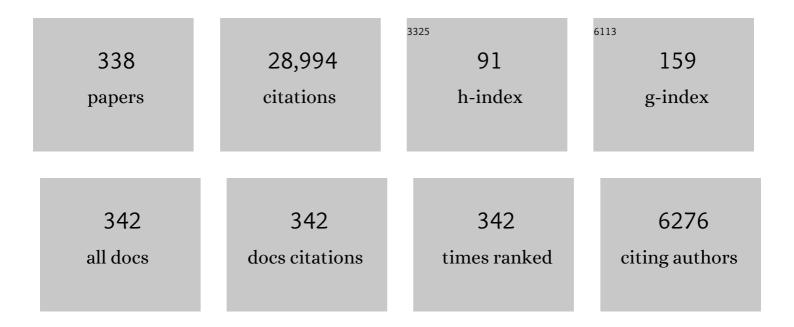
List of Publications by Year in descending order

Source: https://exaly.com/author-pdf/7339842/publications.pdf Version: 2024-02-01



#	Article	IF	CITATIONS
1	Penglai Zircon Megacrysts: A Potential New Working Reference Material for Microbeam Determination of Hf–O Isotopes and U–Pb Age. Geostandards and Geoanalytical Research, 2010, 34, 117-134.	1.7	777
2	Stable isotope geochemistry of ultrahigh pressure metamorphic rocks from the Dabie–Sulu orogen in China: implications for geodynamics and fluid regime. Earth-Science Reviews, 2003, 62, 105-161.	4.0	771
3	Calculation of oxygen isotope fractionation in hydroxyl-bearing silicates. Earth and Planetary Science Letters, 1993, 120, 247-263.	1.8	644
4	Tectonic evolution of a composite collision orogen: An overview on the Qinling–Tongbai–Hong'an–Dabie–Sulu orogenic belt in central China. Gondwana Research, 2013, 23, 1402-1428.	3.0	619
5	Calculation of oxygen isotope fractionation in anhydrous silicate minerals. Geochimica Et Cosmochimica Acta, 1993, 57, 1079-1091.	1.6	588
6	"Calculation of oxygen isotope fractionation in anhydrous silicate minerals.―Geochimica et Cosmochimica Acta. Geochimica Et Cosmochimica Acta, 1993, 57, 3199.	1.6	529
7	Contrasting zircon Hf and O isotopes in the two episodes of Neoproterozoic granitoids in South China: Implications for growth and reworking of continental crust. Lithos, 2007, 96, 127-150.	0.6	510
8	Rift melting of juvenile arc-derived crust: Geochemical evidence from Neoproterozoic volcanic and granitic rocks in the Jiangnan Orogen, South China. Precambrian Research, 2008, 163, 351-383.	1.2	501
9	Metamorphic chemical geodynamics in continental subduction zones. Chemical Geology, 2012, 328, 5-48.	1.4	488
10	Zircon U-Pb and oxygen isotope evidence for a large-scale 180 depletion event in igneous rocks during the Neoproterozoic. Geochimica Et Cosmochimica Acta, 2004, 68, 4145-4165.	1.6	480
11	Zircon U–Pb age, Hf and O isotope constraints on protolith origin of ultrahigh-pressure eclogite and gneiss in the Dabie orogen. Chemical Geology, 2006, 231, 135-158.	1.4	448
12	Distinct mantle sources of low-Ti and high-Ti basalts from the western Emeishan large igneous province, SW China: implications for plume–lithosphere interaction. Earth and Planetary Science Letters, 2004, 228, 525-546.	1.8	439
13	Oxygen isotope fractionation in carbonate and sulfate minerals Geochemical Journal, 1999, 33, 109-126.	0.5	370
14	Zircon U-Pb age and Hf-O isotope evidence for Paleoproterozoic metamorphic event in South China. Precambrian Research, 2006, 151, 265-288.	1.2	359
15	Reworking of juvenile crust: Element and isotope evidence from Neoproterozoic granodiorite in South China. Precambrian Research, 2006, 146, 179-212.	1.2	349
16	Zircon isotope evidence for ≥3.5Ga continental crust in the Yangtze craton of China. Precambrian Research, 2006, 146, 16-34.	1.2	348
17	Zircon U–Pb age and Hf isotope evidence for 3.8ÂGa crustal remnant and episodic reworking of Archean crust in South China. Earth and Planetary Science Letters, 2006, 252, 56-71.	1.8	345
18	Metamorphic effect on zircon Lu–Hf and U–Pb isotope systems in ultrahigh-pressure eclogite-facies metagranite and metabasite. Earth and Planetary Science Letters, 2005, 240, 378-400.	1.8	333

#	Article	IF	CITATIONS
19	A perspective view on ultrahigh-pressure metamorphism and continental collision in the Dabie-Sulu orogenic belt. Science Bulletin, 2008, 53, 3081-3104.	4.3	332
20	Formation and evolution of Precambrian continental lithosphere in South China. Gondwana Research, 2013, 23, 1241-1260.	3.0	317
21	Partial melting, fluid supercriticality and element mobility in ultrahigh-pressure metamorphic rocks during continental collision. Earth-Science Reviews, 2011, 107, 342-374.	4.0	315
22	Chemical geodynamics of continental subduction-zone metamorphism: Insights from studies of the Chinese Continental Scientific Drilling (CCSD) core samples. Tectonophysics, 2009, 475, 327-358.	0.9	299
23	Low-Grade Metamorphic Rocks in the Dabie-Sulu Orogenic Belt: A Passive-Margin Accretionary Wedge Deformed during Continent Subduction. International Geology Review, 2005, 47, 851-871.	1.1	297
24	Subduction zone geochemistry. Geoscience Frontiers, 2019, 10, 1223-1254.	4.3	284
25	U–Pb, Hf and O isotope evidence for two episodes of fluid-assisted zircon growth in marble-hosted eclogites from the Dabie orogen. Geochimica Et Cosmochimica Acta, 2006, 70, 3743-3761.	1.6	271
26	Geochronology and geochemistry of metamorphic rocks in the Jiaobei terrane: Constraints on its tectonic affinity in the Sulu orogen. Precambrian Research, 2007, 152, 48-82.	1.2	254
27	Oxygen and hydrogen isotope geochemistry of ultrahigh-pressure eclogites from the Dabie Mountains and the Sulu terrane. Earth and Planetary Science Letters, 1998, 155, 113-129.	1.8	248
28	Zircon U–Pb age and geochemical constraints on the tectonic affinity of the Jiaodong terrane in the Sulu orogen, China. Precambrian Research, 2008, 161, 389-418.	1.2	246
29	Zircon U–Pb age and trace element evidence for Paleoproterozoic granulite-facies metamorphism and Archean crustal rocks in the Dabie Orogen. Lithos, 2008, 101, 308-322.	0.6	240
30	Low-T eclogite in the Dabie terrane of China: petrological and isotopic constraints on fluid activity and radiometric dating. Contributions To Mineralogy and Petrology, 2004, 148, 443-470.	1.2	237
31	Metamorphic growth and recrystallization of zircon: Distinction by simultaneous in-situ analyses of trace elements, U–Th–Pb and Lu–Hf isotopes in zircons from eclogite-facies rocks in the Sulu orogen. Lithos, 2010, 114, 132-154.	0.6	229
32	Calculation of oxygen isotope fractionation in magmatic rocks. Chemical Geology, 2003, 193, 59-80.	1.4	228
33	Geochemical evidence for interaction between oceanic crust and lithospheric mantle in the origin of Cenozoic continental basalts in east-central China. Lithos, 2009, 110, 305-326.	0.6	219
34	Formation and evolution of Precambrian continental crust in South China. Science Bulletin, 2007, 52, 1-12.	1.7	217
35	Fluid regime in continental subduction zones: petrological insights from ultrahigh-pressure metamorphic rocks. Journal of the Geological Society, 2009, 166, 763-782.	0.9	207
36	Postcollisional magmatism: Geochemical constraints on the petrogenesis of Mesozoic granitoids in the Sulu orogen, China. Lithos, 2010, 119, 512-536.	0.6	205

#	Article	IF	CITATIONS
37	Geochemistry of continental subduction-zone fluids. Earth, Planets and Space, 2014, 66, 93.	0.9	205
38	Developing plate tectonics theory from oceanic subduction zones to collisional orogens. Science China Earth Sciences, 2015, 58, 1045-1069.	2.3	198
39	Experimental melts from crustal rocks: A lithochemical constraint on granite petrogenesis. Lithos, 2016, 266-267, 133-157.	0.6	196
40	The transport of water in subduction zones. Science China Earth Sciences, 2016, 59, 651-682.	2.3	194
41	Continental versus oceanic subduction zones. National Science Review, 2016, 3, 495-519.	4.6	189
42	Remelting of subducted continental lithosphere: Petrogenesis of Mesozoic magmatic rocks in the Dabie-Sulu orogenic belt. Science in China Series D: Earth Sciences, 2009, 52, 1295-1318.	0.9	188
43	Mesozoic mafic magmatism in North China: Implications for thinning and destruction of cratonic lithosphere. Science China Earth Sciences, 2018, 61, 353-385.	2.3	187
44	Oxygen isotope equilibrium between eclogite minerals and its constraints on mineral Sm-Nd chronometer. Geochimica Et Cosmochimica Acta, 2002, 66, 625-634.	1.6	182
45	Zircon U–Pb ages and Hf isotope compositions of migmatite from the North Dabie terrane in China: constraints on partial melting. Journal of Metamorphic Geology, 2007, 25, 991-1009.	1.6	171
46	Carbon and oxygen isotopic covariations in hydrothermal calcites. Mineralium Deposita, 1993, 28, 79.	1.7	169
47	Post-collisional granitoids from the Dabie orogen in China: Zircon U–Pb age, element and O isotope evidence for recycling of subducted continental crust. Lithos, 2007, 93, 248-272.	0.6	169
48	Fluid flow during exhumation of deeply subducted continental crust: zircon U-Pb age and O-isotope studies of a quartz vein within ultrahigh-pressure eclogite. Journal of Metamorphic Geology, 2007, 25, 267-283.	1.6	160
49	Deep Fluids in Subducted Continental Crust. Elements, 2013, 9, 281-287.	0.5	159
50	Neoproterozoic continental accretion in South China: Geochemical evidence from the Fuchuan ophiolite in the Jiangnan orogen. Precambrian Research, 2012, 220-221, 45-64.	1.2	154
51	Melting of subducted continent: Element and isotopic evidence for a genetic relationship between Neoproterozoic and Mesozoic granitoids in the Sulu orogen. Chemical Geology, 2006, 229, 227-256.	1.4	153
52	Zircon U–Pb ages, Hf and O isotopes constrain the crustal architecture of the ultrahigh-pressure Dabie orogen in China. Chemical Geology, 2008, 253, 222-242.	1.4	152
53	Zircon U–Pb age, element and C–O isotope geochemistry of post-collisional mafic-ultramafic rocks from the Dabie orogen in east-central China. Lithos, 2005, 83, 1-28.	0.6	150
54	Syn-exhumation magmatism during continental collision: Evidence from alkaline intrusives of Triassic age in the Sulu orogen. Chemical Geology, 2012, 328, 70-88.	1.4	149

#	Article	IF	CITATIONS
55	Estimation of oxygen diffusivity from anion porosity in minerals Geochemical Journal, 1998, 32, 71-89.	0.5	148
56	Hydrogen and oxygen isotope evidence for fluid–rock interactions in the stages of pre- and post-UHP metamorphism in the Dabie Mountains. Lithos, 1999, 46, 677-693.	0.6	146
57	Regional metamorphism at extreme conditions: Implications for orogeny at convergent plate margins. Journal of Asian Earth Sciences, 2017, 145, 46-73.	1.0	142
58	Element mobility in mafic and felsic ultrahigh-pressure metamorphic rocks during continental collision. Geochimica Et Cosmochimica Acta, 2007, 71, 5244-5266.	1.6	140
59	Trace element and strontium isotope constraints on sedimentary environment of Ediacaran carbonates in southern Anhui, South China. Chemical Geology, 2009, 265, 345-362.	1.4	139
60	Contrasting Lu–Hf and U–Th–Pb isotope systematics between metamorphic growth and recrystallization of zircon from eclogite-facies metagranites in the Dabie orogen, China. Lithos, 2009, 112, 477-496.	0.6	138
61	Fluid history of UHP metamorphism in Dabie Shan, China: a fluid inclusion and oxygen isotope study on the coesite-bearing eclogite from Bixiling. Contributions To Mineralogy and Petrology, 2000, 139, 1-16.	1.2	133
62	Postcollisional mafic igneous rocks record crust-mantle interaction during continental deep subduction. Scientific Reports, 2013, 3, 3413.	1.6	130
63	Extreme 18O depletion in eclogite from the Su-Lu terrane in East China. European Journal of Mineralogy, 1996, 8, 317-324.	0.4	128
64	Fluid inclusions in coesite-bearing eclogites and jadeite quartzite at Shuanghe, Dabie Shan (China). Journal of Metamorphic Geology, 2001, 19, 531-547.	1.6	124
65	Trace elements in zircon and coexisting minerals from low-T/UHP metagranite in the Dabie orogen: Implications for action of supercritical fluid during continental subduction-zone metamorphism. Lithos, 2010, 114, 385-412.	0.6	122
66	Origin of TTG-like rocks from anatexis of ancient lower crust: Geochemical evidence from Neoproterozoic granitoids in South China. Lithos, 2009, 113, 347-368.	0.6	120
67	Triassic granites in South China: A geochemical perspective on their characteristics, petrogenesis, and tectonic significance. Earth-Science Reviews, 2017, 173, 266-294.	4.0	120
68	Geochemical constraints on the genesis of the Bayan Obo Fe–Nb–REE deposit in Inner Mongolia, China. Geochimica Et Cosmochimica Acta, 2009, 73, 1417-1435.	1.6	118
69	Geochemical and U–Pb age constraints on the occurrence of polygenetic titanites in UHP metagranite in the Dabie orogen. Lithos, 2012, 136-139, 93-108.	0.6	116
70	Neoproterozoic anatexis of Archean lithosphere: Geochemical evidence from felsic to mafic intrusions at Xiaofeng in the Yangtze Gorge, South China. Precambrian Research, 2008, 163, 210-238.	1.2	111
71	Dehydration and melting during continental collision: Constraints from element and isotope geochemistry of low-T/UHP granitic gneiss in the Dabie orogen. Chemical Geology, 2008, 247, 36-65.	1.4	111
72	Slab–mantle interaction for thinning of cratonic lithospheric mantle in North China: Geochemical evidence from Cenozoic continental basalts in central Shandong. Lithos, 2012, 146-147, 202-217.	0.6	111

#	Article	IF	CITATIONS
73	TC/EA-MS online determination of hydrogen isotope composition and water concentration in eclogitic garnet. Physics and Chemistry of Minerals, 2007, 34, 687-698.	0.3	110
74	Metamorphic growth and recrystallization of zircons in extremely 18O-depleted rocks during eclogite-facies metamorphism: Evidence from U–Pb ages, trace elements, and O–Hf isotopes. Geochimica Et Cosmochimica Acta, 2011, 75, 4877-4898.	1.6	110
75	Continental subduction channel processes: Plate interface interaction during continental collision. Science Bulletin, 2013, 58, 4371-4377.	1.7	110
76	Distinction between S-type and peraluminous I-type granites: Zircon versus whole-rock geochemistry. Lithos, 2016, 258-259, 77-91.	0.6	109
77	Extreme oxygen isotope signature of meteoric water in magmatic zircon from metagranite in the Sulu orogen, China: Implications for Neoproterozoic rift magmatism. Geochimica Et Cosmochimica Acta, 2008, 72, 3139-3169.	1.6	106
78	Geochemical constraints on the nature of mantle source for Cenozoic continental basalts in east-central China. Lithos, 2011, 125, 940-955.	0.6	106
79	Tectonic driving of Neoproterozoic glaciations: Evidence from extreme oxygen isotope signature of meteoric water in granite. Earth and Planetary Science Letters, 2007, 256, 196-210.	1.8	105
80	Dehydration melting of ultrahighâ€pressure eclogite in the Dabie orogen: evidence from multiphase solid inclusions in garnet. Journal of Metamorphic Geology, 2012, 30, 193-212.	1.6	104
81	Origin of retrograde fluid in ultrahigh-pressure metamorphic rocks: Constraints from mineral hydrogen isotope and water content changes in eclogite–gneiss transitions in the Sulu orogen. Geochimica Et Cosmochimica Acta, 2007, 71, 2299-2325.	1.6	102
82	Origin of postcollisional magmatic rocks in the Dabie orogen: Implications for crust–mantle interaction and crustal architecture. Lithos, 2011, 126, 99-114.	0.6	102
83	Origin of andesitic rocks: Geochemical constraints from Mesozoic volcanics in the Luzong basin, South China. Lithos, 2014, 190-191, 220-239.	0.6	99
84	Oxygen and neodymium isotope evidence for recycling of juvenile crust in northeast China. Geology, 2002, 30, 375.	2.0	98
85	Zircon U-Pb age and o isotope evidence for neoproterozoic low-18O magmatism during supercontinental rifting in South China: Implications for the snowball earth event. Numerische Mathematik, 2008, 308, 484-516.	0.7	98
86	lsotopic constraints on age and duration of fluid-assisted high-pressure eclogite-facies recrystallization during exhumation of deeply subducted continental crust in the Sulu orogen. Journal of Metamorphic Geology, 2006, 24, 687-702.	1.6	97
87	The source of Mesozoic granitoids in South China: Integrated geochemical constraints from the Taoshan batholith in the Nanling Range. Chemical Geology, 2015, 395, 11-26.	1.4	97
88	Zircon isotope evidence for recycling of subducted continental crust in post-collisional granitoids from the Dabie terrane in China. Geophysical Research Letters, 2004, 31, .	1.5	96
89	Petrological, isotopic and fluid inclusion studies of eclogites from Sujiahe, NW Dabie Shan (China). Chemical Geology, 2002, 187, 107-128.	1.4	94
90	Two styles of plate tectonics in Earth's history. Science Bulletin, 2020, 65, 329-334.	4.3	94

#	Article	IF	CITATIONS
91	Transition of UHP eclogites to gneissic rocks of low-amphibolite facies during exhumation: evidence from the Dabie terrane, central China. Lithos, 2003, 70, 269-291.	0.6	93
92	U-Pb ages and trace elements in metamorphic zircon and titanite from UHP eclogite in the Dabie orogen: constraints on P-T-t path. Journal of Metamorphic Geology, 2011, 29, 721-740.	1.6	92
93	Chemical geodynamics of mafic magmatism above subduction zones. Journal of Asian Earth Sciences, 2020, 194, 104185.	1.0	92
94	Mineral isotope evidence for the contemporaneous process of Mesozoic granite emplacement and gneiss metamorphism in the Dabie orogen. Chemical Geology, 2006, 231, 214-235.	1.4	90
95	Fluid Evolution during HP and UHP Metamorphism in Dabie Shan, China: Constraints from Mineral Chemistry, Fluid Inclusions and Stable Isotopes. Journal of Petrology, 2002, 43, 1505-1527.	1.1	89
96	Synexhumation anatexis of ultrahigh-pressure metamorphic rocks: Petrological evidence from granitic gneiss in the Sulu orogen. Lithos, 2013, 156-159, 69-96.	0.6	89
97	Ultrahigh-pressure metamorphic rocks in the Dabie–Sulu orogenic belt: compositional inheritance and metamorphic modification. Geological Society Special Publication, 2019, 474, 89-132.	0.8	89
98	Zircon Hf–O isotope evidence for crust–mantle interaction during continental deep subduction. Earth and Planetary Science Letters, 2011, 308, 229-244.	1.8	86
99	Zircon U–Pb age and Hf isotope evidence for contrasting origin of bimodal protoliths for ultrahighâ€pressure metamorphic rocks from the Chinese Continental Scientific Drilling project. Journal of Metamorphic Geology, 2007, 25, 873-894.	1.6	85
100	A high precision U–Pb age of metamorphic rutile in coesite-bearing eclogite from the Dabie Mountains in central China: a new constraint on the cooling history. Chemical Geology, 2003, 200, 255-265.	1.4	83
101	Termination time of peak decratonization in North China: Geochemical evidence from mafic igneous rocks. Lithos, 2016, 240-243, 327-336.	0.6	83
102	Geochemistry and geochronology of eclogites from the northern Dabie Mountains, central China. Journal of Asian Earth Sciences, 2005, 25, 431-443.	1.0	82
103	Transitional time of oceanic to continental subduction in the Dabie orogen: Constraints from U–Pb, Lu–Hf, Sm–Nd and Ar–Ar multichronometric dating. Lithos, 2009, 110, 327-342.	0.6	82
104	Zircon U–Pb dating of water–rock interaction during Neoproterozoic rift magmatism in South China. Chemical Geology, 2007, 246, 65-86.	1.4	81
105	Zircon Hf–O isotope and whole-rock geochemical constraints on origin of postcollisional mafic to felsic dykes in the Sulu orogen. Lithos, 2012, 136-139, 225-245.	0.6	81
106	The nature of orogenic lithospheric mantle: Geochemical constraints from postcollisional mafic–ultramafic rocks in the Dabie orogen. Chemical Geology, 2012, 334, 99-121.	1.4	79
107	An experimental study of oxygen isotope fractionation between inorganically precipitated aragonite and water at low temperatures. Geochimica Et Cosmochimica Acta, 2003, 67, 387-399.	1.6	78
108	Zircon SHRIMP U–Pb dating, C and O isotopes for impure marbles from the Jiaobei terrane in the Sulu orogen: Implication for tectonic affinity. Precambrian Research, 2006, 144, 1-18.	1.2	78

#	Article	IF	CITATIONS
109	Zr-in-rutile thermometry of eclogite in the Dabie orogen: Constraints on rutile growth during continental subduction-zone metamorphism. Journal of Asian Earth Sciences, 2011, 40, 427-451.	1.0	77
110	Metamorphic zirconology of continental subduction zones. Journal of Asian Earth Sciences, 2017, 145, 149-176.	1.0	77
111	Growth and reworking of cratonic lithosphere. Science Bulletin, 2009, 54, 3347-3353.	4.3	76
112	Remnants of oceanic lower crust in the subcontinental lithospheric mantle: Trace element and Sr–Nd–O isotope evidence from aluminous garnet pyroxenite xenoliths from Jiaohe, Northeast China. Earth and Planetary Science Letters, 2010, 297, 413-422.	1.8	76
113	Temporal relationship between granite cooling and hydrothermal uranium mineralization at Dalongshan in China: a combined radiometric and oxygen isotopic study. Ore Geology Reviews, 2004, 25, 221-236.	1.1	75
114	Petrological and zircon evidence for anatexis of <scp>UHP</scp> quartzite during continental collision in the Sulu orogen. Journal of Metamorphic Geology, 2013, 31, 389-413.	1.6	74
115	Marine carbonate records of terrigenous input into Paleotethyan seawater: Geochemical constraints from Carboniferous limestones. Geochimica Et Cosmochimica Acta, 2014, 141, 508-531.	1.6	74
116	Remnants of premetamorphic fluid and oxygen isotopic signatures in eclogites and garnet clinopyroxenite from the Dabie-Sulu terranes, eastern China. Journal of Metamorphic Geology, 2003, 21, 561-578.	1.6	69
117	Petrogenesis of Triassic granites from the Nanling Range in South China: Implications for geochemical diversity in granites. Lithos, 2014, 210-211, 40-56.	0.6	68
118	Oxygen isotope fractionations involving apatites: Application to paleotemperature determination. Chemical Geology, 1996, 127, 177-187.	1.4	66
119	Oxygen and hydrogen isotope geochemistry of gneisses associated with ultrahigh pressure eclogites at Shuanghe in the Dabie Mountains. Contributions To Mineralogy and Petrology, 1999, 134, 52-66.	1.2	64
120	Tectonic development from oceanic subduction to continental collision: Geochemical evidence from postcollisional mafic rocks in the Hong'an–Dabie orogens. Gondwana Research, 2015, 27, 1236-1254.	3.0	63
121	The tectonic transition from oceanic subduction to continental subduction: Zirconological constraints from two types of eclogites in the North Qaidam orogen, northern Tibet. Lithos, 2016, 244, 122-139.	0.6	63
122	Fluid inclusions in granulites, granulitized eclogites and garnet clinopyroxenites from the Dabie–Sulu terranes, eastern China. Lithos, 2003, 70, 293-319.	0.6	61
123	Introduction to the structures and processes of subduction zones. Journal of Asian Earth Sciences, 2017, 145, 1-15.	1.0	61
124	Oxygen isotope fractionation in hematite and magnetite: A theoretical calculation and application to geothermometry of metamorphic iron-formations. European Journal of Mineralogy, 1991, 3, 877-886.	0.4	60
125	Modification of subcontinental lithospheric mantle above continental subduction zone: Constraints from geochemistry of Mesozoic gabbroic rocks in southeastern North China. Lithos, 2012, 146-147, 164-182.	0.6	59
126	Slab–mantle interaction in continental subduction channel: Geochemical evidence from Mesozoic gabbroic intrusives in southeastern North China. Lithos, 2012, 155, 442-460.	0.6	58

#	Article	IF	CITATIONS
127	Two types of gneisses associated with eclogite at Shuanghe in the Dabie terrane: carbon isotope, zircon U–Pb dating and oxygen isotope. Lithos, 2003, 70, 321-343.	0.6	57
128	Sm–Nd and Rb–Sr dating of pyroxene–garnetite from North Dabie in east-central China: problem of isotope disequilibrium due to retrograde metamorphism. Chemical Geology, 2004, 206, 137-158.	1.4	56
129	Partial equilibrium of radiogenic and stable isotope systems in garnet peridotite during ultrahigh-pressure metamorphism. American Mineralogist, 2003, 88, 1633-1643.	0.9	53
130	Mg–O isotopes trace the origin of Mg-rich fluids in the deeply subducted continental crust of Western Alps. Earth and Planetary Science Letters, 2016, 456, 157-167.	1.8	53
131	Hydrothermal ore deposits in collisional orogens. Science Bulletin, 2019, 64, 205-212.	4.3	53
132	Oxygen isotope fractionation between hydroxide minerals and water. Physics and Chemistry of Minerals, 1998, 25, 213-221.	0.3	52
133	Trace element composition of continentally subducted slabâ€derived melt: insight from multiphase solid inclusions in ultrahighâ€pressure eclogite in the <scp>D</scp> abie orogen. Journal of Metamorphic Geology, 2013, 31, 453-468.	1.6	52
134	The intensity of chemical weathering: Geochemical constraints from marine detrital sediments of Triassic age in South China. Chemical Geology, 2015, 391, 111-122.	1.4	52
135	Continental basalts record the crust-mantle interaction in oceanic subduction channel: A geochemical case study from eastern China. Journal of Asian Earth Sciences, 2017, 145, 233-259.	1.0	51
136	Neoproterozoic granitoid in northwest Sulu and its bearing on the North China-South China Blocks boundary in east China. Geophysical Research Letters, 2004, 31, n/a-n/a.	1.5	50
137	Diffusion compensation for argon, hydrogen, lead, and strontium in minerals: Empirical relationships to crystal chemistry. American Mineralogist, 2007, 92, 289-308.	0.9	50
138	Mineral hydrogen isotopes and water contents in ultrahigh-pressure metabasite and metagranite: Constraints on fluid flow during continental subduction-zone metamorphism. Chemical Geology, 2011, 281, 103-124.	1.4	49
139	Contrasting Lu–Hf isotopes in zircon from Precambrian metamorphic rocks in the Jiaodong Peninsula: Constraints on the tectonic suture between North China and South China. Precambrian Research, 2014, 245, 29-50.	1.2	49
140	The anatectic effect on the zircon Hf isotope composition of migmatites and associated granites. Lithos, 2015, 238, 174-184.	0.6	49
141	Multiple episodes of anatexis in a collisional orogen: Zircon evidence from migmatite in the Dabie orogen. Lithos, 2015, 212-215, 247-265.	0.6	49
142	The crustâ€mantle interaction in continental subduction channels: Zircon evidence from orogenic peridotite in the Sulu orogen. Journal of Geophysical Research: Solid Earth, 2016, 121, 687-712.	1.4	49
143	Carbon concentrations and isotopic ratios of eclogites from the Dabie and Sulu terranes in China. Chemical Geology, 2000, 168, 291-305.	1.4	48
144	Oxygen isotope geochemistry of ultrahigh-pressure metamorphic rocks from 200–4000Âm core samples of the Chinese Continental Scientific Drilling. Chemical Geology, 2007, 242, 51-75.	1.4	48

#	Article	IF	CITATIONS
145	Episodic fluid action during exhumation of deeply subducted continental crust: Geochemical constraints from zoisite–quartz vein and host metabasite in the Dabie orogen. Lithos, 2012, 155, 146-166.	0.6	45
146	Partial melting of deeply subducted continental crust during exhumation: insights from felsic veins and host <scp>UHP</scp> metamorphic rocks in North Qaidam, northern Tibet. Journal of Metamorphic Geology, 2015, 33, 671-694.	1.6	45
147	Oxygen isotope composition of quartz-vein in ultrahigh-pressure eclogite from Dabieshan and implications for transport of high-pressure metamorphic fluid. Physics and Chemistry of the Earth, 2001, 26, 695-704.	0.6	44
148	Oxygen isotope equilibrium between ultrahigh-pressure metamorphic minerals and its constraints on Sm-Nd and Rb-Sr chronometers. Geological Society Special Publication, 2003, 220, 93-117.	0.8	44
149	Extreme Nb/Ta fractionation in metamorphic titanite from ultrahigh-pressure metagranite. Geochimica Et Cosmochimica Acta, 2015, 150, 53-73.	1.6	44
150	Developing the plate tectonics from oceanic subduction to continental collision. Science Bulletin, 2009, 54, 2549-2555.	4.3	43
151	Fluid action on zircon growth and recrystallization during quartz veining within UHP eclogite: Insights from U–Pb ages, O–Hf isotopes and trace elements. Lithos, 2012, 136-139, 126-144.	0.6	43
152	The production of granitic magmas through crustal anatexis at convergent plate boundaries. Lithos, 2021, 402-403, 106232.	0.6	43
153	Mineral oxygen isotope and hydroxyl content changes in ultrahigh-pressure eclogite?gneiss contacts from Chinese Continental Scientific Drilling Project cores. Journal of Metamorphic Geology, 2007, 25, 165-186.	1.6	42
154	Protracted oceanic subduction prior to continental subduction: New Lu-Hf and Sm-Nd geochronology of oceanic-type high-pressure eclogite in the western Dabie orogen. American Mineralogist, 2010, 95, 1214-1223.	0.9	42
155	Multistage growth of garnet in ultrahigh-pressure eclogite during continental collision in the Dabie orogen: Constrained by trace elements and U–Pb ages. Lithos, 2011, 127, 101-127.	0.6	42
156	Geochemical Distinction between Carbonate and Silicate Metasomatism in Generating the Mantle Sources of Alkali Basalts. Journal of Petrology, 2017, 58, 863-884.	1.1	42
157	Multiphase solid inclusions in zoisite-bearing eclogite: evidence for partial melting of ultrahigh-pressure metamorphic rocks during continental collision. Lithos, 2014, 200-201, 1-21.	0.6	41
158	An online method combining a thermal conversion elemental analyzer with isotope ratio mass spectrometry for the determination of hydrogen isotope composition and water concentration in geological samples. Rapid Communications in Mass Spectrometry, 2007, 21, 1386-1392.	0.7	40
159	Stable isotope evidence for involvement of deglacial meltwater in Ediacaran carbonates in South China. Chemical Geology, 2010, 271, 86-100.	1.4	40
160	On the theoretical calculations of oxygen isotope fractionation factors for carbonate-water systems. Geochemical Journal, 2011, 45, 341-354.	0.5	40
161	Zirconological tracing of transition between aqueous fluid and hydrous melt in the crust: Constraints from pegmatite vein and host gneiss in the Sulu orogen. Lithos, 2013, 162-163, 157-174.	0.6	40
162	High temperature glacial meltwater–rock reaction in the Neoproterozoic: Evidence from zircon in-situ oxygen isotopes in granitic gneiss from the Sulu orogen. Precambrian Research, 2016, 284, 1-13.	1.2	40

#	Article	IF	CITATIONS
163	Whole-rock and zircon geochemical distinction between oceanic- and continental-type eclogites in the North Qaidam orogen, northern Tibet. Gondwana Research, 2017, 44, 67-88.	3.0	40
164	Oxygen isotope fractionation in magnetites: structural effect and oxygen inheritance. Chemical Geology, 1995, 121, 309-316.	1.4	39
165	Geochemical insights into the role of metasomatic hornblendite in generating alkali basalts. Geochemistry, Geophysics, Geosystems, 2014, 15, 3762-3779.	1.0	39
166	Tectonic evolution from oceanic subduction to continental collision during the closure of Paleotethyan ocean: Geochronological and geochemical constraints from metamorphic rocks in the Hong'an orogen. Gondwana Research, 2015, 28, 348-370.	3.0	39
167	Petrogenesis of the Mesozoic Shuikoushan peraluminous I-type granodioritic intrusion in Hunan Province, South China: Middle–lower crustal reworking in an extensional tectonic setting. Journal of Asian Earth Sciences, 2016, 123, 224-242.	1.0	39
168	Extreme metamorphism and metamorphic facies series at convergent plate boundaries: Implications for supercontinent dynamics. , 2021, 17, 1647-1685.		39
169	Mössbauer spectroscopy of omphacite and garnet pairs from eclogites: Application to geothermobarometry. American Mineralogist, 2005, 90, 90-100.	0.9	38
170	A geochemical framework for retrieving the linked depositional and diagenetic histories of marine carbonates. Earth and Planetary Science Letters, 2017, 460, 213-221.	1.8	37
171	Isotopic evidence for continental ice sheet in mid-latitude region in the supergreenhouse Early Cretaceous. Scientific Reports, 2013, 3, 2732.	1.6	36
172	Geochemical constraints on the origin of Late Mesozoic andesites from the Ningwu basin in the Middle–Lower Yangtze Valley, South China. Lithos, 2016, 254-255, 94-117.	0.6	36
173	Geochemical constraints on the source nature and melting conditions of Triassic granites from South Qinling in central China. Lithos, 2016, 264, 141-157.	0.6	36
174	Amalgamation of South China into Rodinia during the Grenvillian accretionary orogeny: Geochemical evidence from Early Neoproterozoic igneous rocks in the northern margin of the South China Block. Precambrian Research, 2019, 321, 221-243.	1.2	35
175	Oxygen isotope fractionation in wolframite. European Journal of Mineralogy, 1992, 4, 1331-1336.	0.4	35
176	U–Pb ages and trace elements of metamorphic rutile from ultrahigh-pressure quartzite in the Sulu orogen. Geochimica Et Cosmochimica Acta, 2014, 143, 87-114.	1.6	34
177	Partial melting of the orogenic lower crust: Geochemical insights from post-collisional alkaline volcanics in the Dabie orogen. Chemical Geology, 2017, 454, 25-43.	1.4	34
178	Evidence for regional metamorphism in a continental rift during the Rodinia breakup. Precambrian Research, 2018, 314, 414-427.	1.2	33
179	Geochemical constraints on the protoliths of eclogites and blueschists from North Qilian, northern Tibet. Chemical Geology, 2016, 421, 26-43.	1.4	32
180	Recycling of Paleotethyan oceanic crust: Geochemical record from postcollisional mafic igneous rocks in the Tongbai-Hong'an orogens. Bulletin of the Geological Society of America, 2017, 129, 179-192.	1.6	32

#	Article	IF	CITATIONS
181	Oxygen isotope fractionation in SiO2 and Al2SiO5 polymorphs: effect of crystal structure. European Journal of Mineralogy, 1993, 5, 651-658.	0.4	32
182	Kinetic mechanism of oxygen isotope disequilibrium in precipitated witherite and aragonite at low temperatures: an experimental study. Geochimica Et Cosmochimica Acta, 2002, 66, 63-71.	1.6	31
183	Carbon Isotope Anomaly in Marbles Associated With Eclogites From the Dabie Mountains in China. Journal of Geology, 1998, 106, 97-104.	0.7	30
184	Dehydration and anatexis of <scp>UHP</scp> metagranite during continental collision in the Sulu orogen. Journal of Metamorphic Geology, 2014, 32, 915-936.	1.6	30
185	Source and magma mixing processes in continental subduction factory: Geochemical evidence from postcollisional mafic igneous rocks in the Dabie orogen. Geochemistry, Geophysics, Geosystems, 2015, 16, 659-680.	1.0	30
186	Crust–Mantle Interaction in a Continental Subduction Channel: Evidence from Orogenic Peridotites in North Qaidam, Northern Tibet. Journal of Petrology, 2017, 58, 191-226.	1.1	30
187	Protolith control on fluid availability for zircon growth during continental subduction-zone metamorphism in the Dabie orogen. Journal of Asian Earth Sciences, 2013, 67-68, 93-113.	1.0	29
188	Zircon geochemistry records the action of metamorphic fluid on the formation of ultrahigh-pressure jadeite quartzite in the Dabie orogen. Chemical Geology, 2015, 419, 158-175.	1.4	29
189	Geochronological and geochemical evidence for the nature of the Dongling Complex in South China. Precambrian Research, 2015, 256, 17-30.	1.2	29
190	Slab–Mantle Interaction in the Petrogenesis of Andesitic Magmas: Geochemical Evidence from Postcollisional Intermediate Volcanic Rocks in the Dabie Orogen, China. Journal of Petrology, 2016, 57, 1109-1134.	1.1	29
191	Two episodes of partial melting in ultrahigh-pressure migmatites from deeply subducted continental crust in the Sulu orogen, China. Bulletin of the Geological Society of America, 2016, 128, 1521-1542.	1.6	28
192	Growth of metamorphic and peritectic garnets in ultrahigh-pressure metagranite during continental subduction and exhumation in the Dabie orogen. Lithos, 2016, 266-267, 158-181.	0.6	28
193	The origin of Cenozoic continental basalts in east-central China: Constrained by linking Pb isotopes to other geochemical variables. Lithos, 2017, 268-271, 302-319.	0.6	28
194	Element mobility during continental collision: insights from polymineralic metamorphic vein within UHP eclogite in the Dabie orogen. Journal of Metamorphic Geology, 2013, 31, 221-241.	1.6	27
195	The hydrous properties of subcontinental lithospheric mantle: Constraints from water content and hydrogen isotope composition of phenocrysts from Cenozoic continental basalt in North China. Geochimica Et Cosmochimica Acta, 2014, 143, 285-302.	1.6	27
196	Anomalous nitrogen isotopes in ultrahigh-pressure metamorphic rocks from the Sulu orogenic belt: Effect of abiotic nitrogen reduction during fluid–rock interaction. Earth and Planetary Science Letters, 2014, 403, 67-78.	1.8	27
197	Tracking Fe mobility and Fe speciation in subduction zone fluids at the slab-mantle interface in a subduction channel: A tale of whiteschist from the Western Alps. Geochimica Et Cosmochimica Acta, 2019, 267, 1-16.	1.6	27
198	Hydrogen and oxygen isotope geochemistry of A-type granites in the continental margins of eastern China. Tectonophysics, 2000, 328, 205-227.	0.9	26

#	Article	IF	CITATIONS
199	Geochemical constraints on the origin of post-depositional fluids in sedimentary carbonates of the Ediacaran system in South China. Precambrian Research, 2013, 224, 341-363.	1.2	26
200	Effects of mineral precipitation on the sulfur isotope composition of hydrothermal solutions. Chemical Geology, 1993, 105, 259-269.	1.4	25
201	Experimental studies of oxygen and hydrogen isotope fractionations between precipitated brucite and water at low temperatures. Geochimica Et Cosmochimica Acta, 1999, 63, 2009-2018.	1.6	25
202	Composite carbonate and silicate multiphase solid inclusions in metamorphic garnet from ultrahighâ€ <i>P</i> eclogite in the Dabie orogen. Journal of Metamorphic Geology, 2014, 32, 961-980.	1.6	25
203	Measurement of in-situ oxygen isotope ratios in monazite by SHRIMP ion microprobe: Standards, protocols and implications. Chemical Geology, 2014, 380, 84-96.	1.4	25
204	Carbon isotopes in eclogite and apatite separate from Huangzhen and Shima in SE Dabie. Science in China Series D: Earth Sciences, 2000, 43, 449-457.	0.9	24
205	Geochronology and Stable Isotope Geochemistry of UHP Metamorphic Rocks at Taohang in the Sulu Orogen, East-Central China. International Geology Review, 2007, 49, 259-286.	1.1	24
206	Relationships between O isotope equilibrium, mineral alteration and Rb–Sr chronometric validity in granitoids: implications for determination of cooling rate. Contributions To Mineralogy and Petrology, 2007, 153, 251-271.	1.2	24
207	An online method combining a Gasbench II with continuous flow isotope ratio mass spectrometry to determine the content and isotopic compositions of minor amounts of carbonate in silicate rocks. Rapid Communications in Mass Spectrometry, 2010, 24, 2217-2226.	0.7	24
208	Seeking a geochemical identifier for authigenic carbonate. Nature Communications, 2016, 7, 10885.	5.8	24
209	Oxygen isotope fractionation in double carbonates. Isotopes in Environmental and Health Studies, 2016, 52, 29-46.	0.5	24
210	Geochemical evidence from marine carbonate for enhanced terrigenous input into seawater during the Ediacaran-Cambrian transition in South China. Precambrian Research, 2017, 291, 83-97.	1.2	24
211	Back-reaction of Peritectic Garnet as an Explanation for the Origin of Mafic Enclaves in S-type Granite from the Jiuling Batholith in South China. Journal of Petrology, 2017, 58, 569-598.	1.1	24
212	The three-dimensional Uî—,Pb method: Generalized models and implications for Uî—,Pb two-stage systematics. Chemical Geology, 1992, 100, 3-18.	1.4	23
213	Prediction of high-temperature oxygen isotope fractionation factors between mantle minerals. Physics and Chemistry of Minerals, 1997, 24, 356-364.	0.3	23
214	Formation of metamorphic and metamorphosed garnets in the low-T/UHP metagranite during continental collision in the Dabie orogen. Lithos, 2012, 136-139, 73-92.	0.6	23
215	Polyphase growth of garnet in eclogite from the Hong'an orogen: Constraints from garnet zoning and phase equilibrium. Lithos, 2014, 206-207, 79-99.	0.6	23
216	Tracing subduction zone fluids with distinct Mg isotope compositions: Insights from high-pressure metasomatic rocks (leucophyllites) from the Eastern Alps. Geochimica Et Cosmochimica Acta, 2020, 271, 154-178.	1.6	23

#	Article	IF	CITATIONS
217	Paleoproterozoic tectonic evolution of the northern Yangtze craton from oceanic subduction through continental collision to continental rifting: Geochronological and geochemical records of metabasites from the Tongbai orogen in central China. Precambrian Research, 2020, 350, 105920.	1.2	23
218	Chemical and carbon isotope compositions of fluid inclusions in peridotite xenoliths and eclogites from eastern China: geodynamic implications. Physics and Chemistry of the Earth, 2001, 26, 705-718.	0.6	22
219	<i>In Situ</i> Oxygen Isotope Determination in Serpentine Minerals by Ion Microprobe: Reference Materials and Applications to Ultrahighâ€Pressure Serpentinites. Geostandards and Geoanalytical Research, 2018, 42, 459-479.	1.7	22
220	Geochemical evidence for the production of granitoids through reworking of the juvenile mafic arc crust in the Gangdese orogen, southern Tibet. Bulletin of the Geological Society of America, 2020, 132, 1347-1364.	1.6	22
221	Generation of andesite through partial melting of basaltic metasomatites in the mantle wedge: Insight from quantitative study of Andean andesites. Geoscience Frontiers, 2021, 12, 101124.	4.3	22
222	Geochemical constraints on petrogenesis of marble-hosted eclogites from the Sulu orogen in China. Chemical Geology, 2016, 436, 35-53.	1.4	21
223	Petrological and zircon evidence for the Early Cretaceous granulite-facies metamorphism in the Dabie orogen, China. Lithos, 2017, 284-285, 11-29.	0.6	21
224	Distribution, cycling and impact of water in the Earth's interior. National Science Review, 2017, 4, 879-891.	4.6	21
225	Crustal Metasomatism at the Slabâ€Mantle Interface in a Continental Subduction Channel: Geochemical Evidence From Orogenic Peridotite in the Sulu Orogen. Journal of Geophysical Research: Solid Earth, 2018, 123, 2174-2198.	1.4	21
226	The occurrence of Neoproterozoic low δ180 igneous rocks in the northwestern margin of the South China Block: Implications for the Rodinia configuration. Precambrian Research, 2020, 347, 105841.	1.2	21
227	Garnet geochemistry records the action of metamorphic fluids in ultrahigh-pressure dioritic gneiss from the Sulu orogen. Chemical Geology, 2015, 398, 46-60.	1.4	20
228	The extremely enriched mantle beneath the Yangtze Craton in the Neoproterozoic: Constraints from the Qichun pyroxenite. Precambrian Research, 2016, 276, 194-210.	1.2	20
229	Seismic evidence for the absence of deeply subducted continental slabs in the lower lithosphere beneath the Central Orogenic Belt of China. Tectonophysics, 2018, 723, 178-189.	0.9	20
230	Recycling of Paleo-oceanic crust: Geochemical evidence from Early Paleozoic mafic igneous rocks in the Tongbai orogen, Central China. Lithos, 2019, 328-329, 312-327.	0.6	20
231	Tectonic transition from oceanic subduction to continental collision: New geochemical evidence from Early-Middle Triassic mafic igneous rocks in southern Liaodong Peninsula, east-central China. Bulletin of the Geological Society of America, 2020, 132, 1469-1488.	1.6	20
232	Miocene high-temperature leucogranite magmatism in the Himalayan orogen. Bulletin of the Geological Society of America, 2021, 133, 679-690.	1.6	20
233	Influences of the nature of the initial RbSr system on isochron validity. Chemical Geology: Isotope Geoscience Section, 1989, 80, 1-16.	0.7	19
234	A further three-dimensional U-Pb method for solving the two-stage episodic model Geochemical Journal, 1990, 24, 29-37.	0.5	19

#	Article	IF	CITATIONS
235	Oxygen isotope exchange processes and disequilibrium between calcite and forsterite in an experimental C-O-H fluid. Geochimica Et Cosmochimica Acta, 1999, 63, 1781-1786.	1.6	19
236	Water contents and hydrogen isotopes in nominally anhydrous minerals from UHP metamorphic rocks in the Dabie-Sulu orogenic belt. Science Bulletin, 2013, 58, 4384-4389.	1.7	19
237	The nature of subduction system in the Neoarchean: Magmatic records from the northern Yangtze Craton, South China. Precambrian Research, 2020, 347, 105834.	1.2	19
238	An experimental calibration of oxygen isotope fractionation between calcite and forsterite in the presence of a CO21—,H2O fluid. Chemical Geology, 1994, 116, 17-27.	1.4	18
239	Temperature effect over garnet effect on uptake of trace elements in zircon of TTG-like rocks. Chemical Geology, 2010, 274, 108-125.	1.4	18
240	Fluid-rock interaction and geochemical transport during protolith emplacement and continental collision: A tale from Qinglongshan ultrahigh-pressure metamorphic rocks in the Sulu orogen. Numerische Mathematik, 2014, 314, 357-399.	0.7	18
241	Magma mixing in granite petrogenesis: Insights from biotite inclusions in quartz and feldspar of Mesozoic granites from South China. Journal of Asian Earth Sciences, 2016, 123, 142-161.	1.0	18
242	Zircon geochemical constraints on the protolith nature and metasomatic process of the Mg-rich whiteschist from the Western Alps. Chemical Geology, 2017, 467, 177-195.	1.4	18
243	Mixing of Felsic Magmas in Granite Petrogenesis: Geochemical Records of Zircon and Garnet in Peraluminous Granitoids From South China. Journal of Geophysical Research: Solid Earth, 2018, 123, 2738-2769.	1.4	18
244	On the Direction and Magnitude of Oxygen Isotope Fractionation Between Calcite and Aragonite at Thermodynamic Equilibrium. Aquatic Geochemistry, 2006, 12, 239-268.	1.5	17
245	Polyphase growth of accessory minerals during continental collision: Geochemical evidence from ultrahigh-pressure metamorphic gneisses in the Sulu orogen. Lithos, 2013, 177, 245-267.	0.6	17
246	Zircon evidence for incorporation of terrigenous sediments into the magma source of continental basalts. Scientific Reports, 2018, 8, 178.	1.6	17
247	Geochemical insights into the lithology of mantle sources for Cenozoic alkali basalts in West Qinling, China. Lithos, 2018, 302-303, 86-98.	0.6	17
248	The geochemical nature of mantle sources for two types of Cretaceous basaltic rocks from Luxi and Jiaodong in east-central China. Lithos, 2019, 344-345, 409-424.	0.6	17
249	Origin of arc-like magmatism at fossil convergent plate boundaries: Geochemical insights from Mesozoic igneous rocks in the Middle to Lower Yangtze Valley, South China. Earth-Science Reviews, 2020, 211, 103416.	4.0	17
250	Identification of Jurassic mafic arc magmatism in the eastern North China Craton: Geochemical evidence for westward subduction of the Paleo-Pacific slab. Bulletin of the Geological Society of America, 2020, , .	1.6	17
251	Granulites record the tectonic evolution from collisional thickening to extensional thinning of the Tongbai orogen in central China. Journal of Metamorphic Geology, 2020, 38, 265-295.	1.6	17
252	Phenocryst He–Ar isotopic and whole-rock geochemical constraints on the origin of crustal components in the mantle source of Cenozoic continental basalt in eastern China. Journal of Volcanology and Geothermal Research, 2014, 272, 99-110.	0.8	16

#	Article	IF	CITATIONS
253	Geochemical constraints on the nature of magma sources for Triassic granitoids from South Qinling in central China. Lithos, 2017, 284-285, 30-49.	0.6	16
254	Geochemistry of high-pressure to ultrahigh-pressure granitic melts produced by decompressional melting of deeply subducted continental crust in the Sulu orogen, east-central China. Geochimica Et Cosmochimica Acta, 2020, 288, 214-247.	1.6	16
255	Geochemical evidence for forearc metasomatism of peridotite in the Xigaze ophiolite during subduction initiation in Neo-Tethyan Ocean, south to Tibet. Lithos, 2021, 380-381, 105896.	0.6	16
256	The Effects of Source Mixing and Fractional Crystallization on the Composition of Eocene Granites in the Himalayan Orogen. Journal of Petrology, 2021, 62, .	1.1	16
257	Sulphur isotopic fractionation between sulphate and sulphide in hydrothermal ore deposits: disequilibrium vs equilibrium processes. Terra Nova, 1991, 3, 510-516.	0.9	15
258	Oxygen isotope fractionation between calcite and tremolite: an experimental study. Contributions To Mineralogy and Petrology, 1994, 118, 249-255.	1.2	15
259	Polygenetic titanite records the composition of metamorphic fluids during the exhumation of ultrahighâ€pressure metagranite in the Sulu orogen. Journal of Metamorphic Geology, 2016, 34, 573-594.	1.6	15
260	Migmatites record multiple episodes of crustal anatexis and geochemical differentiation in the Sulu ultrahighâ€pressure metamorphic zone, eastern China. Journal of Metamorphic Geology, 2019, 37, 1099-1127.	1.6	15
261	Fe and O isotopes in coesite-bearing jadeite quartzite from the Western Alps record multistage fluid-rock interactions in a continental subduction zone. Geochimica Et Cosmochimica Acta, 2021, 312, 1-24.	1.6	15
262	Relict zircon U-Pb age and O isotope evidence for reworking of Neoproterozoic crustal rocks in the origin of Triassic S-type granites in South China. Lithos, 2018, 300-301, 261-277.	0.6	15
263	Chemical synthesis of CaCO3 minerals at low temperatures and implication for mechanism of polymorphic transition. Neues Jahrbuch Fur Mineralogie, Abhandlungen, 2001, 176, 323-343.	0.1	15
264	Crustal thickening and continental formation in the Neoarchean: Geochemical records by granitoids from the Taihua Complex in the North China Craton. Precambrian Research, 2021, 367, 106446.	1.2	15
265	Tourmaline boron isotopes trace metasomatism by serpentinite-derived fluid in continental subduction zone. Geochimica Et Cosmochimica Acta, 2022, 320, 122-142.	1.6	15
266	Geochemical constraints on the nature of Late Archean basaltic-andesitic magmatism in the North China Craton. Earth-Science Reviews, 2022, 230, 104065.	4.0	15
267	Early archean inheritance in zircon from Mesozoic dalongshan granitoids in the Yangtze Foldbelt of Southeast China Geochemical Journal, 1990, 24, 133-141.	0.5	14
268	Compensation effect for electrical conductivity and its applications to estimate oxygen diffusivity in minerals. Journal of Geophysical Research, 2003, 108, .	3.3	14
269	Postcollisional mafic igneous rocks record recycling of noble gases by deep subduction of the continental crust. Lithos, 2016, 252-253, 135-144.	0.6	14
270	Oxygen and carbon isotope anomalies in the ultrahigh pressure metamorphic rocks of the Dabie-Sulu terranes: implications for geodynamics. Episodes, 1997, 20, 104-108.	0.8	14

#	Article	IF	CITATIONS
271	Geochemical evidence for partial melting of progressively varied crustal sources for leucogranites during the Oligocene–Miocene in the Himalayan orogen. Chemical Geology, 2022, 589, 120674.	1.4	14
272	Oxygen isotope exchange and disequilibrium between calcite and tremolite in the absence and presence of an experimental C?O?H fluid. Contributions To Mineralogy and Petrology, 2004, 146, 683-695.	1.2	13
273	Geochemical insights from clinopyroxene phenocrysts into the effect of magmatic processes on petrogenesis of intermediate volcanics. Lithos, 2018, 316-317, 137-153.	0.6	13
274	The Origin of Garnets in Anatectic Rocks from the Eastern Himalayan Syntaxis, Southeastern Tibet: Constraints from Major and Trace Element Zoning and Phase Equilibrium Relationships. Journal of Petrology, 2019, 60, 2241-2280.	1.1	13
275	Metamorphism in Subduction Zones. , 2021, , 612-622.		13
276	Effect of polymorphic transition on oxygen isotope fractionation between aragonite, calcite, and water: A low-temperature experimental study. American Mineralogist, 2005, 90, 1121-1130.	0.9	12
277	Diverse P–T paths of the northern Dabie complex in central China and its reworking in the early Cretaceous. Journal of Asian Earth Sciences, 2011, 42, 633-640.	1.0	12
278	Exhumation of Ultrahigh-Pressure Metamorphic Terranes. , 2021, , 868-878.		12
279	Geochemistry of vein and wallrock carbonates from the Ediacaran system in South China: Insights into the origins of depositional and post-depositional fluids. Chemical Geology, 2015, 404, 71-87.	1.4	11
280	Syn-exhumation magmatism in an active continental margin above a continental subduction zone: Evidence from Late Triassic mafic igneous rocks in the southeastern North China Block. Bulletin of the Geological Society of America, 2021, 133, 1267-1282.	1.6	11
281	Carbon concentration and isotope composition of granites from Southeast China. Physics and Chemistry of the Earth, 2001, 26, 821-833.	0.6	10
282	An oxygen isotope study of quartz veins within eclogites from the Dabie terrane. Science in China Series D: Earth Sciences, 2001, 44, 621-634.	0.9	10
283	Geochemical evidence from coesite-bearing jadeite quartzites for large-scale flow of metamorphic fluids in a continental subduction channel. Geochimica Et Cosmochimica Acta, 2019, 265, 354-370.	1.6	10
284	Geochemical constraints on the origin of Neoarchean magmatic rocks in the Lüliang Complex, North China Craton: Tectonic implications. Precambrian Research, 2019, 327, 212-231.	1.2	10
285	Zircon evidence for the Eoarchean (~3.7â€ ⁻ Ga) crustal remnant in the Sulu Orogen, eastern China. Precambrian Research, 2020, 337, 105529.	1.2	10
286	Convergent Plate Boundaries and Accretionary Wedges. , 2021, , 770-787.		10
287	Oxygen isotope fractionation in phosphates: the role of dissolved complex anions in isotope exchange ^{â€} . Isotopes in Environmental and Health Studies, 2016, 52, 47-60.	0.5	9
288	Water in garnet pyroxenite from the Sulu orogen: Implications for crust-mantle interaction in continental subduction zone. Chemical Geology, 2018, 478, 18-38.	1.4	9

#	Article	IF	CITATIONS
289	Syn-exhumation melting of the subducted continental crust: Geochemical evidence from early Paleozoic granitoids in North Qaidam, northern Tibet. Lithos, 2020, 374-375, 105707.	0.6	9
290	The accretion history of the South China Block at its northwest margin in the Neoproterozoic: Records from the Changba complex in the Mianlue zone. Precambrian Research, 2021, 352, 106006.	1.2	9
291	Partial melting of subducted continental crust: Geochemical evidence from synexhumation granite in the Sulu orogen. Bulletin of the Geological Society of America, 0, , .	1.6	8
292	Syn-exhumation magmatism during continental collision: Geochemical evidence from the early Paleozoic Fushui mafic rocks in the Qinling orogen, Central China. Lithos, 2020, 352-353, 105318.	0.6	8
293	Geochemical Distinction Between Altered Oceanic Basalt- and Seafloor Sediment-Derived Fluids in the Mantle Source of Mafic Igneous Rocks in Southwestern Tianshan, Western China. Journal of Petrology, 2021, 62, .	1.1	8
294	Origin of syn-collisional granitoids in the Gangdese orogen: Reworking of the juvenile arc crust and the ancient continental crust. Bulletin of the Geological Society of America, 2022, 134, 577-598.	1.6	8
295	Peritectic minerals record partial melting of the deeply subducted continental crust in the Sulu orogen. Journal of Metamorphic Geology, 2022, 40, 87-120.	1.6	8
296	Barium isotope fractionation during dehydration melting of the subducting oceanic crust: Geochemical evidence from OIB-like continental basalts. Chemical Geology, 2022, 594, 120751.	1.4	8
297	Tectonic switch from a lithospheric rift to an active continental margin in the Paleoproterozoic: Evidence from low l´180 granites from the Trans-North China Orogen in the North China Craton. Precambrian Research, 2022, 377, 106672.	1.2	8
298	On the use of a three-dimensional method in solving the U-Pb two-stage model Geochemical Journal, 1989, 23, 37-43.	0.5	7
299	The Meyer-Neldel compensation law for electrical conductivity in olivine. Applied Physics Letters, 2005, 87, 252116.	1.5	7
300	Fifty years of plate tectonics. National Science Review, 2018, 5, 119-119.	4.6	7
301	Geochemical evidence for reworking of the juvenile crust in the Neoarchean for felsic magmatism in the Yunzhongshan area, the North China Craton. Precambrian Research, 2019, 335, 105493.	1.2	7
302	Geochemical Evidence for Hydration and Dehydration of Crustal Rocks During Continental Rifting. Journal of Geophysical Research: Solid Earth, 2019, 124, 12593-12619.	1.4	7
303	A missing piece between Laurentia and the North China Craton in Rodinia: Evidence from metasedimentary rocks of the North Qinling Terrane in central China. Precambrian Research, 2021, 361, 106246.	1.2	7
304	An Experimental Study of Partial Melting of Metafelsic Rocks: Constraints on the Feature of Anatectic Melts and the Origin of Garnets in Collisional Orogens. Journal of Earth Science (Wuhan, China), 2022, 33, 753-769.	1.1	7
305	The effect of crystal fractionation on the geochemical composition of syn-exhumation magmas: Implication for the formation of high Î ⁻ 56Fe granites in collisional orogens. Geochimica Et Cosmochimica Acta, 2022, 332, 156-185.	1.6	7
306	Postcollisional flow of aqueous fluid within ultrahigh-pressure eclogite in the Dabie orogen. Journal of Geochemical Exploration, 2006, 89, 115-118.	1.5	6

#	Article	IF	CITATIONS
307	Isotopic disequilibrium in ultrahigh-pressure and retrograde metamorphism of eclogite and gneiss from the Chinese Continental Scientific Drilling in the Sulu orogen, China: evidence from mineral Nd–Sr–O isotopic composition. International Journal of Earth Sciences, 2010, 99, 727-743.	0.9	6
308	Enhanced weathering as a trigger for the rise of atmospheric O2 level from the late Ediacaran to the early Cambrian. Scientific Reports, 2019, 9, 10630.	1.6	6
309	Magnesium-carbon isotopes trace carbon recycling in continental subduction zone. Lithos, 2020, 376-377, 105774.	0.6	6
310	Plate Tectonics. , 2021, , 744-758.		6
311	Source diversity in controlling the compositional diversity of Cenozoic granites in the Tethyan Himalaya. Lithos, 2021, 388-389, 106072.	0.6	6
312	Metapelites record two episodes of decompressional metamorphism in the Himalayan orogen. Lithos, 2021, 394-395, 106183.	0.6	6
313	Oxygen isotope fractionation between calcite and forsterite formed via reaction from dolomite and tremolite at 680°C. European Journal of Mineralogy, 1994, 6, 179-186.	0.4	6
314	Oxygen isotope fractionation in zinc oxides and implications for zinc mineralization in the Sterling Hill deposit, USA. Mineralium Deposita, 1996, 31, 98.	1.7	5
315	Response to the Comment by J. Horita and R.N. Clayton on "The studies of oxygen isotope fractionation between calcium carbonates and water at low temperaturesâ€. Geochimica Et Cosmochimica Acta, 2007, 71, 3136-3143.	1.6	5
316	Mesozoic reworking of the Paleozoic subducted continental crust beneath the south-central margin of the North China Block: Geochemical evidence from granites in the Xiaoqinling-Xiong'ershan region. Lithos, 2020, , 105886.	0.6	5
317	Construction of <i>P</i> – <i>T</i> – <i>t</i> paths for eclogite in the Tongbai orogen by combining phase equilibria modelling with zircon inclusion composition. Journal of Metamorphic Geology, 2021, 39, 947-976.	1.6	5
318	Fluid-present and fluid-absent melting of muscovite in migmatites in the Himalayan orogen: Constraints from major and trace element zoning and phase equilibrium relationships. Lithos, 2021, 388-389, 106071.	0.6	5
319	Discussion on the use of \hat{l}' - \hat{l}'' diagram in interpreting stable isotope data. European Journal of Mineralogy, 1992, 4, 635-644.	0.4	5
320	Continental crust recycling in ancient oceanic subduction zone: Geochemical insights from arc basaltic to andesitic rocks and paleo-trench sediments in southern Tibet. Lithos, 2022, 414-415, 106619.	0.6	5
321	Decoupling between Mg and Ca isotopes in alkali basalts: Implications for geochemical differentiation of subduction zone fluids. Chemical Geology, 2022, 606, 120983.	1.4	5
322	Precise carbon isotopic ratio analyses of micro amounts of carbonate and nonâ€carbonate in basalt using continuousâ€flow isotope ratio mass spectrometry. Rapid Communications in Mass Spectrometry, 2018, 32, 48-56.	0.7	4
323	Whole-rock geochemical and zircon Hf–O isotopic constraints on the origin of granitoids and their mafic enclaves from the Triassic Mishuling pluton in West Qinling, central China. Journal of Asian Earth Sciences, 2020, 189, 104136.	1.0	4
324	The compositional variation of I-type granites: Constraints from geochemical analyses and phase equilibrium calculations for granites from the Qinling orogen, central China. Journal of Asian Earth Sciences, 2020, 200, 104471.	1.0	4

#	Article	IF	CITATIONS
325	Fluid activity during exhumation of deep-subducted continental plate. Science Bulletin, 2004, 49, 985.	1.7	4
326	Comment on "Pb-isotopic evidence for U-Th-Pb behaviour in a prograde amphibolite to granulite facies transition from the Lewisian complex of north-west Scotland: Implication for Pb-Pb dating―by M. J. Whitehouse. Geochimica Et Cosmochimica Acta, 1990, 54, 1835-1838.	1.6	3
327	Petrogenesis of continental igneous rocks: Reply to the comment by Qiu et al. on "Origin of TTG-like rocks from anatexis of ancient lower crust: Geochemical evidence from Neoproterozoic granitoids in South China [Lithos 113 (2009) 347–368]― Lithos, 2010, 116, 191-194.	0.6	3
328	A common crustal component in the sources of bimodal magmatism: Geochemical evidence from Mesozoic volcanics in the Middle-Lower Yangtze Valley, South China. Bulletin of the Geological Society of America, 0, , .	1.6	3
329	Zircon and titanite behaviors during partial melting of metabasite in the post-collisional stage: Constraints from garnet pyroxenite in the Dabie orogen, China. Journal of Asian Earth Sciences, 2021, 205, 104615.	1.0	3
330	Contrasting zircon and garnet behaviors during metamorphic transformation from eclogite to granulite facies: Constraints from orogenic metabasites from North Qaidam in northern Tibet. Journal of Asian Earth Sciences, 2021, 220, 104924.	1.0	2
331	Elevation of zircon Hf isotope ratios during crustal anatexis: Evidence from migmatites close to the eastern Himalayan syntaxis in southeastern Tibet. Lithos, 2022, 412-413, 106592.	0.6	2
332	25 years of continental deep subduction. Science Bulletin, 2009, 54, 4266-4270.	1.7	1
333	China and Mongolia—Precambrian-Paleozoic. , 2021, , 494-508.		1
334	Geochemistry of polygenetic titanite traces metamorphic and anatectic processes during the exhumation of deeply subducted continental crust. Lithos, 2021, 398-399, 106314.	0.6	1
335	Low H2O/Ce ratios and δ18O values for continental basalts in eastern China: Geochemical evidence for involvement of the dehydrated crustal component in the mantle source. Lithos, 2021, 400-401, 106339.	0.6	1
336	Response of trace elements to partial melting of felsic crust at high to ultrahigh temperatures: Implications for granite geochemistry. Lithos, 2022, 422-423, 106743.	0.6	1
337	Comment and Reply on "Sulfur isotopic ratios of the magnetite-series and ilmenite-series granitoids of the Sierra Nevada batholith—A reconnaissance study". Geology, 1990, 18, 671.	2.0	0
338	Magma differentiation and recharge in the petrogenesis of early paleozoic mafic intrusives in the Qilian orogen, northwestern China. Lithos, 2021, , 106492.	0.6	0